Clinical Cancer Research

Shallow Whole Genome Sequencing on Circulating Cell-Free DNA Allows Reliable Noninvasive Copy-Number Profiling in Neuroblastoma Patients

Nadine Van Roy[1,2], Malaïka Van Der Linden[1,3], Björn Menten[1], Annelies Dheedene[1], Charlotte Vandeputte[1,2], Jo Van Dorpe[3], Geneviève Laureys[2,4], Marleen Renard[5], Tom Sante[1], Tim Lammens[2,4], Bram De Wilde[2,4], Frank Speleman[1,2], and Katleen De Preter[1,2]

Abstract

Purpose: Neuroblastoma (NB) is a heterogeneous disease characterized by distinct clinical features and by the presence of typical copy-number alterations (CNAs). Given the strong association of these CNA profiles with prognosis, analysis of the CNA profile at diagnosis is mandatory. Therefore, we tested whether the analysis of circulating cell-free DNA (cfDNA) present in plasma samples of patients with NB could offer a valuable alternative to primary tumor DNA for CNA profiling.

Experimental Design: In 37 patients with NB, cfDNA analysis using shallow whole genome sequencing (sWGS) was compared with arrayCGH analysis of primary tumor tissue.

Results: Comparison of CNA profiles on cfDNA showed highly concordant patterns, particularly in high-stage patients. Numerical chromosome imbalances as well as large and focal structural aberrations including *MYCN* and *LIN28B* amplification and *ATRX* deletion could be readily detected with sWGS using a low input of cfDNA.

Conclusions: In conclusion, sWGS analysis on cfDNA offers a cost-effective, noninvasive, rapid, robust and sensitive alternative for tumor DNA copy-number profiling in most patients with NB.
Clin Cancer Res; 23(20); 6305–14. ©2017 AACR.

Introduction

Neuroblastoma (NB) is the most common extracranial solid tumor of childhood and is characterized by a remarkable biological and clinical heterogeneity ranging from spontaneous regression (stage 4s) to overt metastasis (1, 2). Recurrent somatic mutations are rare in NB, while DNA copy-number alterations (CNAs) are present in almost all cases (3–7). The distinct patterns of CNAs in favorable (whole chromosome imbalances only) versus highly aggressive NBs (segmental chromosomal gains and losses) have led to the mandatory inclusion of multi-locus assays for CNA profiling for the genetic work-up of new patients with NB at diagnosis (6, 7). To this purpose, either fluorescence in situ hybridization (FISH), multiplex ligation-dependent probe amplification (MLPA), arrayCGH, or SNParray was used (8, 9). However, all these methods depend on the availability of primary tumor tissue at diagnosis, which can be obtained only through an invasive procedure. Open surgical biopsies are preferred, but often diagnosis relies on tru-cut or fine-needle biopsies. However, these small biopsies only provide a genomic view of one particular small area of a primary tumor, while NB tumors are known to demonstrate intratumoral, spatial, and temporal heterogeneity (10–13).

During the last few years, it has become evident that circulating tumor cells or circulating free nucleic acids present in peripheral blood or plasma can be used as a valuable alternative to biopsy. These so-called liquid biopsies can be used for diagnosis, monitoring therapy response, or prediction of relapse and allow frequent disease monitoring without additional risk and burden for the patients (14–16). Especially targeted approaches on liquid biopsies have allowed the detection of specific mutations or methylation events, while whole genome studies so far are relatively scarce (17). In NB, liquid biopsies have already shown to be useful to detect *MYCN* amplification and *ALK* mutations using real-time quantitative PCR and digital droplet PCR (18, 19). Thus far, for NB only one single study compared primary NB tumor DNA and cfDNA using a classical copy-number profiling technique (i.e., arrayCGH) (20).

In this study, we report on the first successful application of shallow whole genome sequencing (sWGS) for the detection of CNAs in cfDNA of 37 patients with NB. CNA profiles generated

[1]Center for Medical Genetics, Ghent University, Ghent, Belgium. [2]Cancer Research Institute Ghent, Ghent University, Ghent, Belgium. [3]Department of Pathology, Ghent University, Ghent, Belgium. [4]Department of Pediatric Hematology-Oncology and Stem Cell Transplantation, Ghent University Hospital, Ghent, Belgium. [5]Department of Pediatric Hematology-Oncology and Stem Cell Transplantation, Leuven University Hospital, Leuven, Belgium.

Note: Supplementary data for this article are available at Clinical Cancer Research Online (http://clincancerres.aacrjournals.org/).

Corresponding Author: Katleen De Preter, Center for Medical Genetics, UZ Gent, De Pintelaan 185, 9000 Gent, Belgium. Phone: 329-332-5533; Fax: 329-332-6549; E-mail: katleen.depreter@ugent.be

doi: 10.1158/1078-0432.CCR-17-0675

Translational Relevance

Neuroblastoma (NB) is an aggressive childhood tumor with low mutational burden and characterized by typical copy-number alterations (CNAs) used to co-guide treatment decisions. Here, we show the feasibility of noninvasive detection of CNAs using shallow whole genome sequencing (sWGS) of cell-free DNA (cfDNA) from plasma from patients with NB with or without metastatic disease. Interestingly, using this approach, we also detected aberrations that were not observed in the tumor biopsy. Given the importance of establishing a CNA profile at diagnosis for therapeutic stratification and the fact that in many patients primary tumor material is often very limited or even unavailable, we propose to include this low-cost WGS approach in the genetic work-up of patients with NB at diagnosis. Moreover, the proposed method offers the perspective for noninvasive genomic testing at several time points over the treatment course without additional risk and burden for the patient.

from cfDNA isolated from as little as 200 μL plasma were compared with genomic profiles of the corresponding tumors determined by standard array technology.

Materials and Methods

Patient material

The local ethical committee approved the study and written consent was obtained from all patients enrolled in this study or their representatives. The clinical characteristics of the patients are summarized in Table 1 and Supplementary Table S1. In total, plasma samples were obtained from 12 low-stage (including two stage 4s) and 25 patients with high-stage NB, including 13 *MYCN*-amplified cases.

Blood sample collection, plasma preparation, and cfDNA extraction

Whole blood samples from all patients with NB were collected in EDTA vacutainer tubes (BD Biosciences) and kept at 4°C until further processing. Plasma was prepared within 24 hours after blood collection. Plasma was obtained after 1 × 10 min centrifugation at 1,600 rcf at 4°C, centrifuge acceleration, and deceleration was set to two, followed by a subsequent centrifugation step of 1 × 10 minutes at 16,000 rcf at 4°C. The plasma was stored at −80°C (21 samples) or was processed immediately for subsequent cfDNA extraction (16 samples). cfDNA was extracted using the QIAamp Circulating Nucleic Acid Kit (Qiagen). The Qiagen kit was used in conjunction with the QiaVac 24 plus vacuum manifold (Qiagen). Isolation of cfDNA was done starting from 1 to 3.5 mL of plasma, if less plasma was available, volumes were adjusted by adding of 1× PBS. For 21 of 37 samples the input of plasma was 200 μL. DNA extraction was performed according to the manufacturer's instructions. In case of <3.5 mL starting volume of plasma, all volumes of the ingredients in the kit were adjusted accordingly. DNA was eluted in 50 μL of AVE buffer (Qiagen). DNA concentration was measured using the Qubit high-sensitivity kit (Thermo Fisher Scientific). Size distribution of the cfDNAs was measured using the Fragment analyzer (Advanced Analytical) according to the manufacturer's instructions.

Shallow depth WGS of cfDNA

Shallow depth WGS (sWGS) of cfDNA was performed using an Ion Proton sequencer (Thermo Fisher Scientific), starting from 5 ng input of cfDNA using the protocol as previously described (21). The minimal number of reads per sample was set at 10 million (mean coverage of 0.4×). Four tumors (cases 5, 13, 15, and 16) were also analyzed using sWGS on the HiSeq 3000 (Illumina Inc.), starting from 200 ng input of tumor DNA according to the manufacturer's instructions. Using a bin size of 100 kb, the R-Bioconductor package QDNAseq (22) was applied to visualize the DNA copy-number profile and call genomic aberrations. Each genome profile (line view and chromosome view) was manually checked for aberrations. All profiles were visualized using the online tool Vivar (http://cmgg.be/vivar/; ref. 23).

ArrayCGH analysis of tumor tissue and DTC samples

For those patients with NB that lacked tumor biopsy material at diagnosis, disseminated NB cells (DTCs) present in the bone marrow were isolated using magnetic activated cell sorting as previously described (24).

DNA from primary tumors or DTCs was isolated using the DNeasy blood and tissue kit (Qiagen) according to the manufacturer's instructions. Tumor samples or DTCs were profiled on a custom-designed 180K array (Agilent Technologies) as previously described (25). Tumor DNA and control DNA (400 ng) were labeled using the random prime labeling (BioPrime ArrayCGH genomic labeling system, Thermo Fisher Scientific) with Cy3 and Cy5 dyes (Perkin Elmer), respectively. Processing was performed according to the manufacturer's instructions (Agilent Technologies). Slides were scanned with an Agilent scanner (G2505C, Agilent Technologies) and data extracted using the feature Extraction v10.1.1.1 software program (Agilent Technologies), profiles were visualized using the Vivar platform (http://cmgg.be/vivar/; ref. 23). ArrayCGH profiles were further processed with the "no waves" and circular binary segmentation (CBS) algorithm (26, 27).

Data mining and statistics

Data-mining and statistical analysis was performed in R statistical environment (R-version 3.2.1), including *t*-tests, Mann–Whitney tests, histograms (stats package), and boxplots (ggplot2 package). With the function normalmixEM (mixtools package), mixed model fitting on the histograms of the copy-number data was performed. From these fits, the mean and the standard deviation of the different distributions (for gains, normal copy-number, and deletions) was calculated, followed by z-score calculation, that is, ('mean signal for normal copy number' – 'mean signal for altered copy number')/('standard deviation of the signal for the alteration').

With the samtools view function, the distribution of the read lengths was retrieved. After normalization of the read length distribution data, the histograms for the different samples were plotted and compared in R.

qPCR analysis of LIN28B

To validate the *LIN28B* amplification, qPCR was performed as described by De Preter and colleagues (28). For *LIN28B*, both primers were designed with Primer 3 version 0.4.0 (http://bioinfo.ut.ee/primer3-0.4.0) using the standard parameters of this software. The following primer sequences were used for

Table 1. Summary information table of 37 patients with neuroblastoma included in this study

Case number	INSS stage	Age at diagnosis (months)	Metastasis	MYCN status	TumorDNA genomic profile	cfDNA genomic profile
1	4	19	Yes	MNA	Segmental	Segmental
2	4	60	Yes	No MNA	Flat	Flat
3	4	68	Yes	MNA	Segmental	Segmental
4	4	69	Yes	No MNA	Segmental	Segmental
5	4s	3	Yes	No MNA	Numerical	Numerical
6	1	13	No	No MNA	Segmental	Flat
7	4	39	Yes	No MNA	Segmental	Segmental
8	4	50	Yes	MNA	Segmental	Segmental
9	4	44	Yes	No MNA	Segmental	Segmental
10	4s	2	Yes	No MNA	Numerical	Flat
11	4	46	Yes	No MNA	Segmental	Segmental
12	1	13	No	MNA	Segmental	Segmental
13	4	32	Yes	No MNA	Segmental	Segmental
14	4	44	Yes	No MNA	Segmental	Segmental
15	4	21	Yes	MNA	Segmental	Segmental
16	1	1	No	No MNA	Numerical	Numerical
17	3	9	No	No MNA	Numerical	Numerical
18	1	2	Yes	No MNA	Numerical	Flat
19	1	4	No	No MNA	Numerical	Flat
20	1	16	No	No MNA	Numerical	Flat
21	1	2	No	No MNA	Numerical	Flat
22	4	11	Yes	No MNA	Segmental	Flat
23	4	71	Yes	MNA	Segmental	Segmental
24	1	51	No	No MNA	Segmental	Flat
25	4	52	Yes	No MNA	Segmental	Segmental
26	4	5	Yes	MNA	Segmental	Segmental
27	4	20	Yes	MNA	Segmental	Segmental
28	4	25	Yes	MNA	Segmental	Segmental
29	1	1	No	No MNA	Numerical	Flat
30	4	25	Yes	MNA	Segmental	Segmental
31	4	18	Yes	MNA	Segmental	Segmental
32	4	9	Yes	No MNA	Numerical	Segmental
33	3	37	No	MNA	Segmental	Segmental
34	4	4	Yes	No MNA	Segmental	Flat
35	4	15	Yes	MNA	Segmental	Segmental
36	4	22	Yes	No MNA	Segmental	Segmental
37	1	12	No	No MNA	Segmental	Flat

MNA: *MYCN* amplification.

LIN28B: forward primer 5′ AATACTGGGCATTACCTCCCAAC 3′ and reverse primer 5′ ATCAGTGTGGGCGGTACAAAA 3′.

Normalization was done using two reference genes, *BCMA* and *SDC4*. These genes are respectively located at 16p13 and 20q13, both chromosomal regions that rarely show genetic abnormalities in NB.

All reactions were performed in duplicate and NGP was used as a positive control as this cell line was shown to have a focal gain of *LIN28B* by arrayCGH.

Results

Quality assessment of cfDNA from plasma

In this study, circulating cell-free DNA (cfDNA) was isolated from plasma of 37 patients with NB (Table 1). Plasma from patients with cancer showed significantly ($P < 0.01$) higher cfDNA yields ranging from 17 to 7,500 ng/mL plasma (median: 194 ng/mL) as compared with the cfDNA yields in the plasma of normal controls (#=8) and pregnant women (#=100; Fig. 1A). Interestingly, we could also show that sufficient cfDNA could be isolated for sWGS (i.e., 5 ng) starting from only 200 μL of plasma.

Comparison of the size distribution of the sWGS reads showed that the cfDNA reads generated in cancer patients were smaller than these from healthy individuals (pregnant women; $P =$ 1.32E−3 when comparing the median read lengths) as previously shown (refs. 29, 30; Fig. 1B and C).

Setting the parameters for copy-number profile analysis from shallow WGS data

The most important parameter to be set for QDNAseq analysis is the bin size, which also determines the resolution for detection of CNAs (22). Therefore, we analyzed the copy-number profile of a case with three different bin sizes (i.e., 15 kb, 50 kb, and 100 kb) (Fig. 2). After model fitting on the histograms of the copy-number data, we calculated z-scores to determine how well deleted and gained regions are discriminated from regions without genomic aberrations. The z-score represents how many standard deviations the mean signal for aberrant regions deviates from the mean signal for nonaberrant regions. sWGS data analyzed at 100 kb bin size have z-scores that match with clear identification of gains and losses, comparable as in the arrayCGH copy-number data (z-scores around 3 for gains and 5 for losses).

Comparison of copy-number profiles obtained using sWGS on plasma cfDNA versus arrayCGH on primary tumor DNA

In total, cfDNA genomic profiles from plasma and corresponding primary tumor profiles from 37 patients with NB

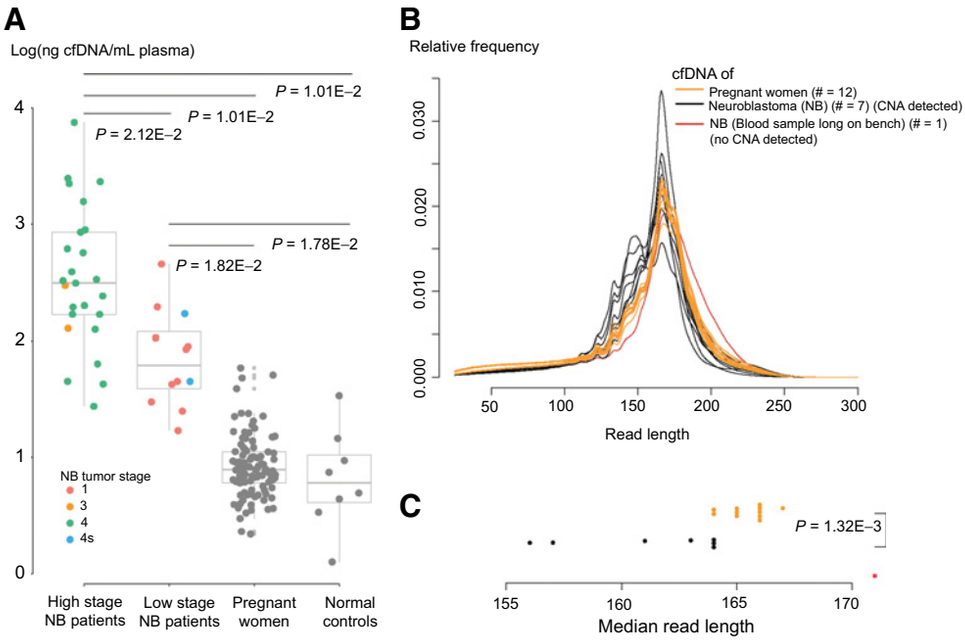

Figure 1.

A, cfDNA concentration in plasma of patients with NB is significantly higher than in plasma samples of pregnant women and plasma samples of healthy individuals (*P* values measured with *t* test are indicated), (**B–C**) the size distribution of read lengths (**B**) and median read length (**C**) measured on cfDNA of patients with NB (#=9, black) is smaller than that of pregnant women (#=12, orange). One sample from a patient with NB that was left over the weekend on the bench before plasma isolation shows larger fragments (red).

were established using sWGS and conventional oligonucleotide arrayCGH, respectively (Table 1). A detailed overview of all aberrations that were identified in the tumor tissue and in the corresponding cfDNA can be found in Supplementary Table S1 and Supplementary Fig. S2. For one case, tumor tissue was not available and DTCs were used instead. We confirmed a segmental aberrant profile in the cfDNA in 22 out of 26 cases presenting with segmental aberrations in the tumor DNA (Fig. 3A and B). Twenty-one of these 22 cases belong to the high-stage tumors, while one case was a low-stage tumor (case 12). In the cfDNA of the remaining four cases, we identified no copy-number changes. For two of these cases, it could be explained by the fact that peripheral blood was obtained 1 month after diagnosis and after therapy (both cases showed negative MIBG scans at that moment).

In addition, a typical profile with only whole chromosome imbalances was detected in three out of 10 cases presenting with only numerical aberrations in the tumor DNA (Fig. 3C). From the 10 cases presenting with only numerical aberrations in the tumor DNA, two cases belonged to the high-stage group, whereas eight cases were low-stage patients. One out of the three cases presenting with only numerical aberrations in the cfDNA belonged to the high-stage group. In the cfDNA of six of the other cases no copy-number changes could be identified, while in one case (case 32) we identified segmental aberrations at chromosome 11 (del(11)(p15.5p12),dup(11)(p12q14.1), del(11)(q14.1q25)) in the cfDNA in addition to the numerical aberrations that were also present in the tumor DNA. In one case (case 2), a flat profile for both the tumor and the cfDNA was observed.

Detection of amplifications and other focal aberrations in cfDNA

Given the importance of focal CNAs that target specific genes in relation to therapeutic stratification and/or tumor biology, we further zoomed in on focal copy-number amplifications/gains and deletions (aberrations <3 Mb). Amplifications, in particular those encompassing the *MYCN* locus, are known to infer a poor prognosis in patients with NB (31, 32). Accurate assessment of *MYCN* is thus of utmost importance in the genetic work-up of the primary tumor as it may directly impact treatment decisions. Importantly, in this study, all *MYCN* amplifications observed by arrayCGH in 13 tumor DNA samples were also detected in cfDNA. Furthermore, a chromosome 5p amplicon containing *IRX1/IRX2* (5p15.33, ±2,430 kb) (case 30) as well as a focal gain of the *CCDC148/PKP4* locus (2q24.1, ±240 kb; case 15) was detected both in the cfDNA and tumor tissue. Remarkably, in case 8, a *LIN28B* amplification was only present in the cfDNA while not detected in the tumor DNA, suggesting possible tumor heterogeneity (6q16.3-6q21, ±2.7 Mb).

Next, we investigated in more detail focal deletions targeting one or a small number of genes (<1 Mb). *ATRX* deletions are known to mark a specific subset of NB tumors with an alternative telomere lengthening (ALT) phenotype (5, 33, 34). In this series, a focal *ATRX* deletion (Xq21.1, ±800 kb) was detected in both the cfDNA and the tumor DNA of one patient (case 7). In addition, a focal *AUTS2* deletion (7q11.22, ±820 kb) was detected in both DNA fractions of another case (case 14). In contrast, three other focal aberrations including a *CDKN2A/B* homozygous deletion (case 3) (9p21.3, ±190 kb), a *PTPRD* deletion (case 7) (9p24.1, ±320 kb), and a small 12q-deletion (*USP15*, *MON2*, *PPM1H*, and

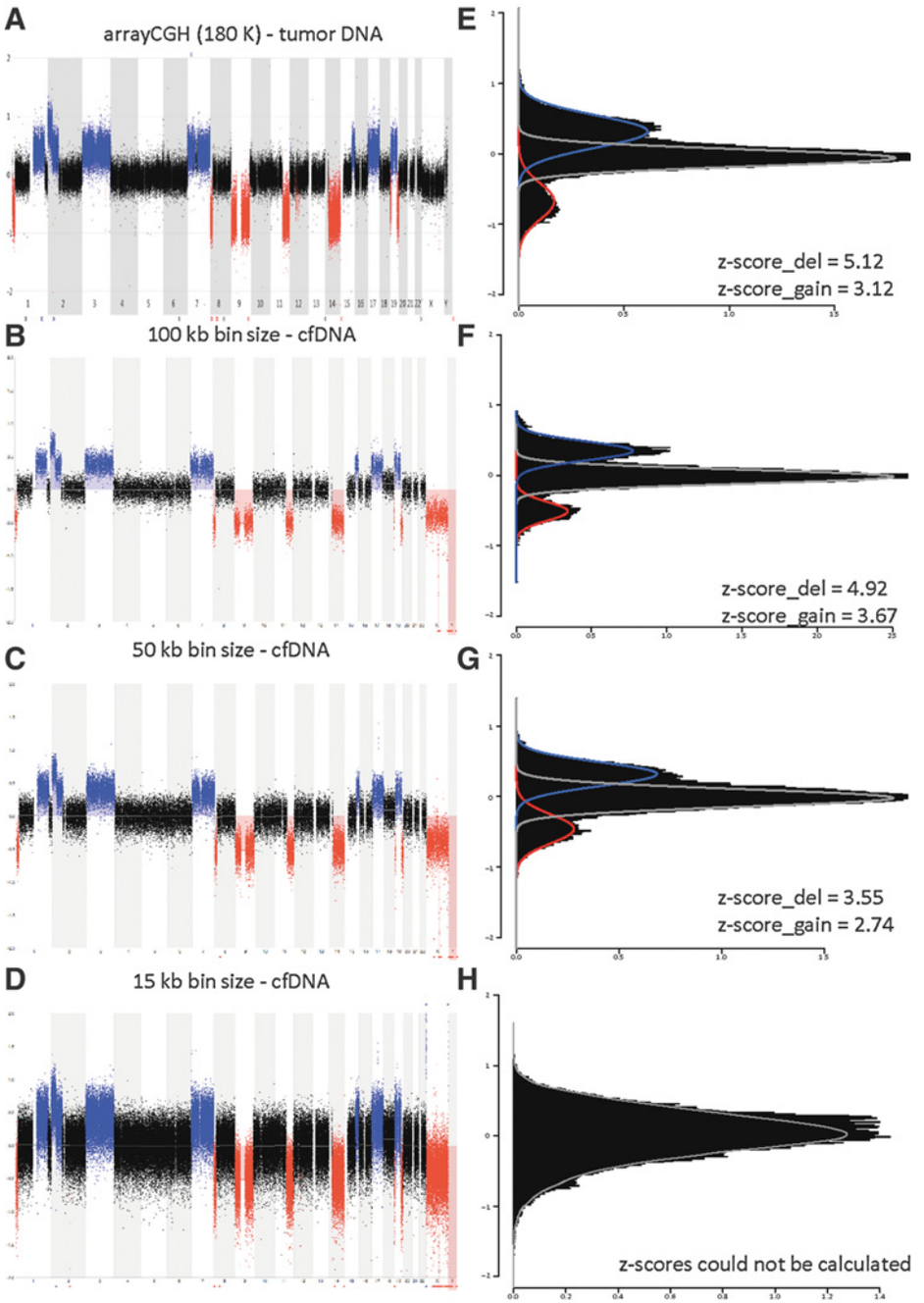

Figure 2.
Comparison of copy-number profiles of cfDNA obtained using different bin sizes [100 kb (**B**), 50 kb (**C**), 15 kb (**D**)] with a matching arrayCGH profile of the primary tumor (**A**). Based on the models fitted on the frequency plots of the copy-number alterations, z-scores to detect gains or losses can be measured and compared in the different profiles (**E**–**H**).

AVPR1A) (case 9) (12q14.1/12q14.2, ±850 kb) that were detected in the tumor DNA could not be detected in the cfDNA using 100 kb binning. Interestingly, the ∼190 kb *CDKN2A/B* focal homozygous deletion could be detected in the cfDNA sWGS data by using a smaller bin size (15 kb), while the other two focal deletions remained undetectable at this resolution.

Capturing spatial and temporal tumor heterogeneity with cfDNA sWGS

An interesting observation from our study was the finding that noninvasive cfDNA analysis in several cases provided additional information regarding the spatial and temporal tumor heterogeneity of the primary tumor (and possibly metastases) at diagnosis and relapse. Indeed, in 13 cases, additional genomic alterations were observed in the cfDNA compared with the tumor DNA. Remarkably, in some cases (like cases 7 and 13), these additional alterations were detected at lower copy-number level than the shared alterations (Fig. 4), suggesting that these alterations are only present in subclones. In contrast, in five tumors we detected aberrations in the tumor tissue that were not present in the cfDNA.

To rule out that these discordances can be attributed to the use of two different technologies (i.e., arrayCGH and sWGS),

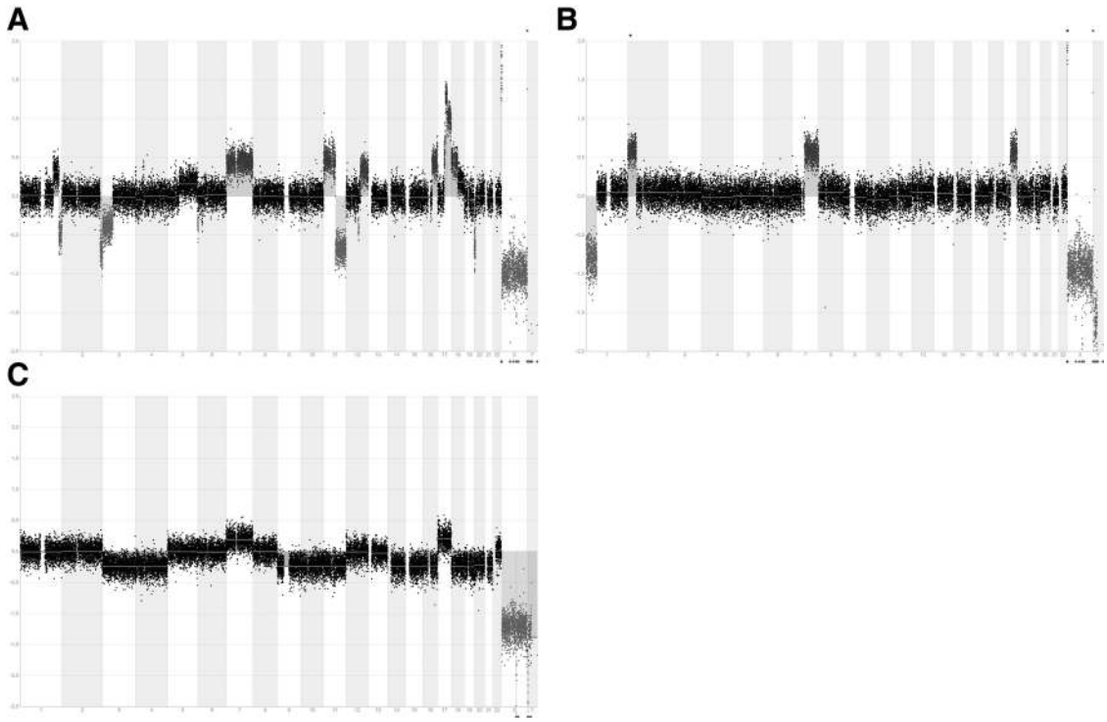

Figure 3.
Copy-number profiles of tumors with typical segmental (**A**, **B**) and numerical (**C**) alterations measured on cfDNA from plasma using sWGS.

the copy-number profile of four tumors (cases 5, 13, 15, and 16) was examined with both technologies, and no differences were observed (Supplementary Fig. S1).

In addition to spatial heterogeneity, cfDNA also allows to noninvasively capture temporal heterogeneity. For one case (case 8), cfDNA was available both at diagnosis and at relapse (1 year after diagnosis; Fig. 5). The cfDNA at diagnosis showed some extra segmental as well as numerical aberrations in comparison with the tumor tissue, including an amplification of the *LIN28B* gene. At relapse, this amplicon was not present anymore in the cfDNA, but the profile at relapse contained additional segmental alterations such as del(4)(q31.3q35.2), dup(9)(q31.3q33.1), dup(10)(p15.3p11.21), and del(17)(q11.2q21.2). This observation was confirmed using independent qPCR based copy-number quantification (Supplementary Fig. S3).

Discussion

We describe the feasibility to reliably detect copy-number aberrations using sWGS on cfDNA isolated from plasma of NB patients. While several studies already reported on the use of cfDNA for the detection of mutations (35, 36), copy-number analysis on liquid biopsies has been rarely attempted (17, 18, 37, 38). Shallow whole genome or low pass sequencing have been described for the detection of copy-number analysis in cfDNA in the context of prostate cancer, lung cancer, and ovarian cancer (39–42). In NB, however, this is the first report on the use of sWGS analysis on cfDNA and the comparison with arrayCGH profiles generated on the corresponding tumor tissue or disseminated tumor cells. Easier scoring and the apparently lack of wave patterns in the sWGS profiles of the cfDNA and four tumor samples is striking, although sWGS and arrayCGH profiles are not exactly comparable due to differences in resolution. We could successfully determine the copy-number profile on 25 out of 35 cfDNA NB samples isolated from blood taken at diagnosis. Although cfDNA profiling was successful in a minority of low-stage localized tumors (four out of nine), copy-number profiles could mainly be determined in the cfDNA of patients with high-stage, metastasizing tumors (18 out of 19), which is in line with the results of Chicard and colleagues (20). Most of the measures are very comparable between both studies; however, some quality measures are a little bit lower in our study, but this can be explained by the different sample-set composition, that is, in the Chicard study, less low-stage, nonmetastasized samples (stages 1, 2) (13/66 = 20%) were included compared with our study (10/37 = 27%). It is well appreciated that in patients with low-stage, nonmetastasizing tumors, lower amounts of (tumor derived) cfDNA are detected. This is supported by the lower cfDNA concentrations in blood of low-stage patients. This finding is in line with other studies (19, 20, 43). In case 6, sWGS of the cfDNA revealed a flat profile despite very high cfDNA concentration. This discordance can be explained by the fact that the peripheral blood stored in an EDTA tube was kept over weekend before plasma isolation, resulting in lysis of the white blood cells and leading to contamination of the cfDNA with constitutional DNA, as previously described (44). This and previous reports thus underline the importance of good cfDNA sample work-up protocols for successful downstream analyses.

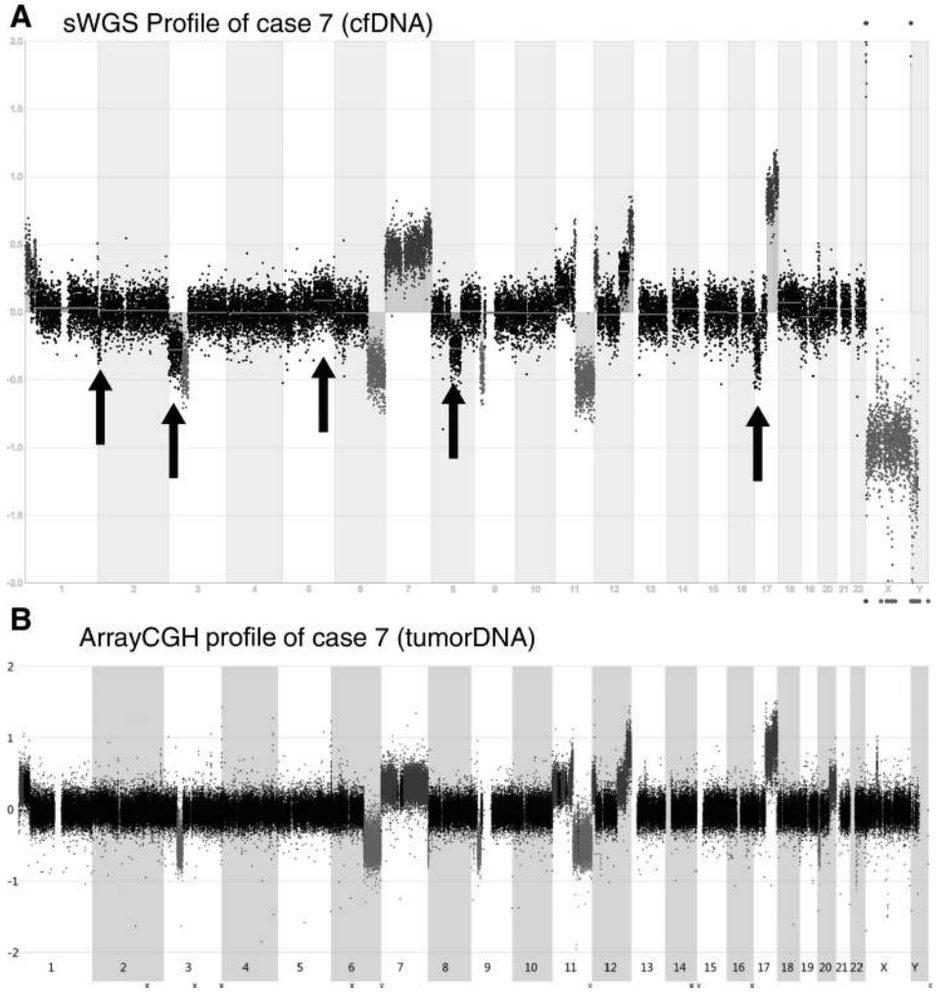

Figure 4.
Copy-number profiles of NB cases analysed using sWGS on cfDNA (**A**) identifies additional alterations at subclonal level, that is, alterations measured at different copy-number level as compared with the alterations also observed in the tumor DNA (arrayCGH; **B**).

Determination of *MYCN* amplification status is important because it is a biomarker strongly associated with unfavorable outcome of NB disease (31, 32). *MYCN* amplification detection has already been described in cfDNA, but most of these studies relied on real-time quantitative PCR or digital droplet PCR (18, 45–47). Our sWGS platform allowed the identification of *MYCN* amplification in all 13 cases with described *MYCN* amplification in the tumor cells. In addition, other focal copy-number aberrations associated with clinical outcome such as *ATRX* and *CDKN2A/B* deletion (5, 33, 34, 48) could be identified in the cfDNA. Another important prognostic biomarker is the presence of segmental CNAs being associated with poor survival outcome (6, 7). In 22 out of 24 cases, a copy-number profile with segmental aberrations was confirmed using sWGS on cfDNA. In three out of 11 cases, sWGS of cfDNA confirmed the presence of only numerical alterations. Interestingly, in one case with only numerical aberrations in the tumor sample, the cfDNA presented with additional segmental aberrations at chromosome 11 (case 32).

The relatively high occurrence of tumor heterogeneity is further demonstrated by the presence of alterations in the cfDNA that could not be detected in the tumor tissue in half of the cases (13 out of 25 cases where a nonflat profile was detected in the cfDNA). Detailed examination of these aberrations showed that some of these might only be present at the subclonal level. These findings underscore the problems associated with the availability of small biopsies, since they do not accurately represent the whole tumor. Furthermore, these results indicate that cfDNA analysis better reflects the spatial tumor heterogeneity present in a single patient as previously described (12, 13). However, alterations that were identified in the tissue DNA remained undetected in the cfDNA of five cases. Among others, we could not detect the presence of a small deletion encompassing the *PTPRD* gene. Optimization of the data-mining pipeline using z-score analysis or increasing read depth might help to detect such small CNAs. The applied sWGS procedure on cfDNA, as described in this project, uses the same workflow as our routinely performed NIPT (noninvasive prenatal testing) analysis for aneuploidy detection (21), which allows rapid and routine profiling of cfDNAs from patients with NB. While standard NIPT protocols start from 3.5 mL plasma, we found that reduced cfDNA input from plasma samples as little as 200 μL plasma were sufficient for successful analysis. The use of such small samples is particularly important for very young patients with NB, given the smaller blood volumes that can be sampled. Furthermore, compared with the previously reported array-based Oncoscan platform for which at least 20 to 50 ng of cfDNA is needed (20), sWGS only requires as little as 5 ng of

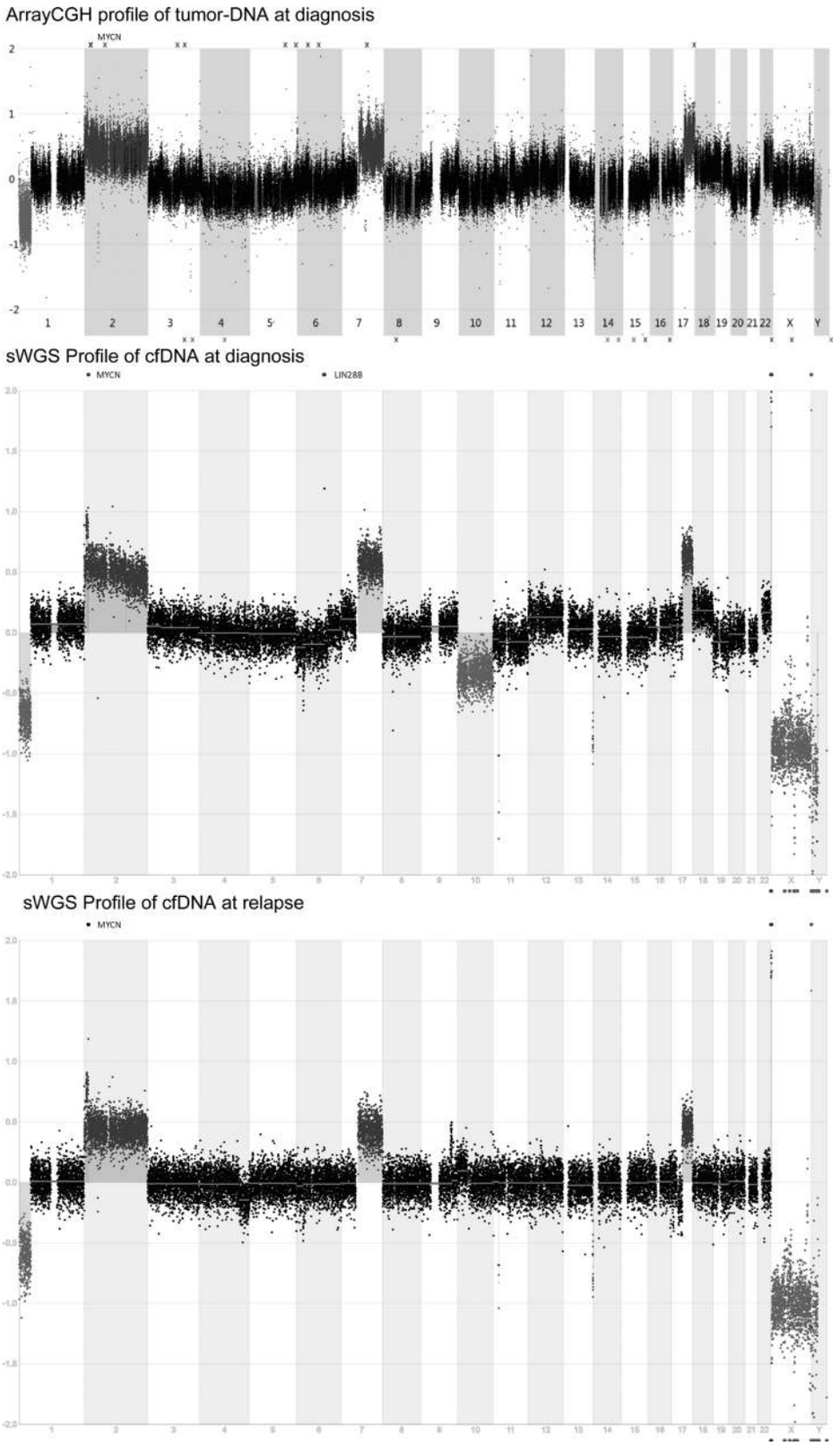

Figure 5.
Temporal copy-number heterogeneity measured in cfDNA of one patient at diagnosis and at relapse. The top panel represents the arrayCGH profile of the tumor at diagnosis.

cfDNA. Further advantages of sWGS profiling are the cost-effective procedure with a comparable price to arrayCGH and the fact that this sequencing-based method can be easily integrated in the workflow of contemporary molecular diagnostic laboratories, within a time frame of 21 calendar days.

In conclusion, we demonstrate the feasibility of sWGS to detect copy-number aberrations from a small input of plasma and cfDNA in a series of patients with NB representing all tumor stages. This is of special interest in clinical management of patients with NB, as these patients are often very young at diagnosis and biopsies are generally very small or cannot be performed. We therefore propose to include this low-cost WGS approach in the genetic work-up of patients with NB at diagnosis. For high-stage patients, cfDNA analysis could offer an alternative to analysis of scarce and small tumor biopsies; however, for most low-stage tumors, DNA analysis of the tumor biopsy will still be mandatory, but in these cases tumor availability is in general not a problem. Optimization and fine-tuning of the data-mining pipeline is warranted to allow detection of all present alterations including small alterations and homozygous deletions. Future plans will also be directed toward the identification of mutations in a selected panel of genes on cfDNA in patients with NB and toward the mapping of the temporal tumor heterogeneity. The sensitive detection of mutations, however, requires other techniques such as digital droplet PCR and duplex sequencing (49, 50). Indeed, a major advantage of liquid biopsies is that they are obtained noninvasively in the patient and therefore offers the possibility to do serial analyses: at diagnosis, during therapy, and at relapse (12, 13, 51, 52).

Disclosure of Potential Conflicts of Interest

No potential conflicts of interest were disclosed.

Authors' Contributions

Conception and design: N. Van Roy, B. Menten, G. Laureys, B. De Wilde, F. Speleman, K. De Preter

Development of methodology: B. Menten, A. Dheedene, F. Speleman, K. De Preter

Acquisition of data (provided animals, acquired and managed patients, provided facilities, etc.): N. Van Roy,C. Vandeputte, J. Van Dorpe, G. Laureys, M. Renard, T. Lammens, B. De Wilde, K. De Preter

Analysis and interpretation of data (e.g., statistical analysis, biostatistics, computational analysis): N. Van Roy, B. Menten, C. Vandeputte, T. Sante, F. Speleman, K. De Preter

Writing, review, and/or revision of the manuscript: N. Van Roy, M. Van Der Linden, B. Menten, C. Vandeputte, J. Van Dorpe, G. Laureys, T. Lammens, B. De Wilde, F. Speleman, K. De Preter

Administrative, technical, or material support (i.e., reporting or organizing data, constructing databases): N. Van Roy, M. Van Der Linden, B. Menten, A. Dheedene, C. Vandeputte, M. Renard, T. Sante, T. Lammens, F. Speleman, K. De Preter

Study supervision: N. Van Roy, B. Menten, G. Laureys, F. Speleman, K. De Preter

Acknowledgments

We are thankful for the technical assistance of Peter Degrave, Geert De Vos, Dimitri Broucke, Tamara Declercq, Isabel Brisard, Shalina Baute, Tine De Pretre, and Melek Yoruk.

Grant Support

The authors would like to thank the following funding agencies: the Belgian Foundation against Cancer (project 2015-146) to F. Speleman, the Flemish liga against cancer (B/14651/01 and STIVLK2016000601), Ghent University (BOF16/GOA/23) to F. Speleman, the Belgian Program of Interuniversity Poles of Attraction (IUAP Phase VII - P7/03) to F. Speleman, the Fund for Scientific Research Flanders (Research project G021415N) to K. De Preter and project 18B1716N to B. De Wilde, the European Union H2020 (OPTIMIZE-NB GOD9415N and TRANSCAN-ON THE TRAC GOD8815N) to F. Speleman. The Ghent University Hospital innovation project for molecular pathology (project number: KW/1694/PAN/001/001) to J. Van Dorpe and M. Van Der Linden, vzw Kinderkankerfonds, a nonprofit childhood cancer foundation under Belgian law to T. Lammens. Grant from Ghent University (Multidisciplinary Research Partnership "Bioinformatics: from nucleotides to networks," 01MR0410) to B. Menten and A. Dheedene.

The costs of publication of this article were defrayed in part by the payment of page charges. This article must therefore be hereby marked *advertisement* in accordance with 18 U.S.C. Section 1734 solely to indicate this fact.

Received March 8, 2017; revised June 2, 2017; accepted July 10, 2017; published OnlineFirst July 14, 2017.

References

1. Matthay KK, Maris JM, Schleiermacher G, Nakagawara A, Mackall CL, Diller L, et al. Neuroblastoma. Nat Rev Dis Primers 2016;2:16078.
2. Louis CU, Shohet JM. Neuroblastoma: molecular pathogenesis and therapy. Annu Rev Med 2015;66:49–63.
3. Sausen M, Leary RJ, Jones S, Wu J, Reynolds CP, Liu X, et al. Integrated genomic analyses identify ARID1A and ARID1B alterations in the childhood cancer neuroblastoma. Nat Genet 2013;45:12–7.
4. Pugh TJ, Morozova O, Attiyeh EF, Asgharzadeh S, Wei JS, Auclair D, et al. The genetic landscape of high-risk neuroblastoma. Nat Genet 2013;45:279–84.
5. Molenaar JJ, Koster J, Zwijnenburg DA, van Sluis P, Valentijn LJ, van der Ploeg I, et al. Sequencing of neuroblastoma identifies chromothripsis and defects in neuritogenesis genes. Nature 2012;483:589–93.
6. Schleiermacher G, Mosseri V, London WB, Maris JM, Brodeur GM, Attiyeh E, et al. Segmental chromosomal alterations have prognostic impact in neuroblastoma: a report from the INRG project. Br J Cancer 2012;107:1418–22.
7. Janoueix-Lerosey I, Schleiermacher G, Michels E, Mosseri V, Ribeiro A, Lequin D, et al. Overall genomic pattern is a predictor of outcome in neuroblastoma. J Clin Oncol 2009;27:1026–33.
8. Combaret V, Iacono I, Bréjon S, Schleiermacher G, Pierron G, Couturier J, et al. Analysis of genomic alterations in neuroblastoma by multiplex ligation-dependent probe amplification and array comparative genomic hybridization: a comparison of results. Cancer Genet 2012;205:657–64.
9. Ambros IM, Brunner B, Aigner G, Bedwell C, Beiske K, Bénard J, et al. A multilocus technique for risk evaluation of patients with neuroblastoma. Clin Cancer Res 2011;17:792.
10. Squire JA, Thorner P, Marrano P, Parkinson D, Ng YK, Gerrie B, et al. Identification of mycn copy number heterogeneity by direct fish analysis of neuroblastoma preparations. Mol Diagn 1996;1:281–9.
11. Ambros PF, Ambros IM, Kerbl R, Luegmayr A, Rumpler S, Ladenstein R, et al. Intratumoural heterogeneity of 1p deletions and MYCN amplification in neuroblastomas. Med Pediatr Oncol 2001;36:1–4.
12. Berbegall AP, Navarro S, Noguera R. Diagnostic implications of intrapatient genetic tumor heterogeneity. Mol Cell Oncol 2016;3:e1079671.
13. Bogen D, Brunner C, Walder D, Ziegler A, Abbasi R, Ladenstein RL, et al. The genetic tumor background is an important determinant for heterogeneous MYCNamplified neuroblastoma. Int J Cancer 2016;139:153–63.
14. Montagut C, Siravegna G, Bardelli A. Liquid biopsies to evaluate early therapeutic response in colorectal cancer. Ann Oncol 2015;26:1525–7.
15. Luke JJ, Oxnard GR, Paweletz CP, Camidge DR, Heymach JV, Solit DB, et al. Realizing the potential of plasma genotyping in an age of genotype-directed therapies. J Natl Cancer Inst 2014;106:dju214–dju.

16. Murtaza M, Dawson S-J, Tsui DWY, Gale D, Forshew T, Piskorz AM, et al. Non-invasive analysis of acquired resistance to cancer therapy by sequencing of plasma DNA. Nature 2013;497:108–12.
17. Heitzer E, Ulz P, Geigl JB, Speicher MR. Non-invasive detection of genome-wide somatic copy number alterations by liquid biopsies. Mol Oncol 2016;10:494–502.
18. Combaret V, Audoynaud C, Iacono I, Favrot M-C, Schell M, Bergeron C, et al. Circulating MYCN DNA as a tumor-specific marker in neuroblastoma patients. Cancer Res 2002;62:3646.
19. Combaret V, Iacono I, Bellini A, Bréjon S, Bernard V, Marabelle A, et al. Detection of tumor ALK status in neuroblastoma patients using peripheral blood. Cancer Med 2015;4:540–50.
20. Chicard M, Boyault S, Colmet Daage L, Richer W, Gentien D, Pierron G, et al. Genomic copy number profiling using circulating free tumor DNA highlights heterogeneity in neuroblastoma. Clin Cancer Res 2016; 22:5564.
21. Dheedene A, Sante T, De Smet M, Vanbellinghen J-F, Grisart B, Vergult S, et al. Implementation of noninvasive prenatal testing by semiconductor sequencing in a genetic laboratory. Prenat Diagn 2016;36:699–707.
22. Scheinin I, Sie D, Bengtsson H, van de Wiel MA, Olshen AB, van Thuijl HF, et al. DNA copy number analysis of fresh and formalin-fixed specimens by shallow whole-genome sequencing with identification and exclusion of problematic regions in the genome assembly. Genome Res 2014;24:2022–32.
23. Sante T, Vergult S, Volders P-J, Kloosterman WP, Trooskens G, De Preter K, et al. ViVar: a comprehensive platform for the analysis and visualization of structural genomic variation. PLoS One 2014;9:e113800.
24. Vandewoestyne M, Kumps C, Swerts K, Menten B, Lammens T, Philippé J, et al. Isolation of disseminated neuroblastoma cells from bone marrow aspirates for pretreatment risk assessment by array comparative genomic hybridization. Int J Cancer 2012;130:1098–108.
25. Kumps C, Fieuw A, Mestdagh P, Menten B, Lefever S, Pattyn F, et al. Focal DNA copy number changes in neuroblastoma target MYCN regulated genes. PLoS One 2013;8:e52321.
26. van de Wiel MA, Brosens R, Eilers PHC, Kumps C, Meijer GA, Menten B, et al. Smoothing waves in array CGH tumor profiles. Bioinformatics 2009; 25:1099–104.
27. Olshen AB, Venkatraman ES, Lucito R, Wigler M. Circular binary segmentation for the analysis of arraybased DNA copy number data. Biostatistics 2004;5:557–72.
28. De Preter K, Speleman F, Combaret V, Lunec J, Laureys G, Eussen BHJ, et al. Quantification of MYCN, DDX1, and NAG gene copy number in neuroblastoma using a real-time quantitative PCR assay. Mod Pathol 2002;15: 159–66.
29. Underhill HR, Kitzman JO, Hellwig S, Welker NC, Daza R, Baker DN, et al. Fragment length of circulating tumor DNA. PLoS Genet 2016;12: e1006162.
30. Mouliere F, Robert B, Arnau Peyrotte E, Del Rio M, Ychou M, Molina F, et al. High fragmentation characterizes tumour-derived circulating DNA. PLoS One 2011;6:e23418.
31. Brodeur GM, Seeger RC, Schwab M, Varmus HE, Bishop JM. Amplification of N-myc in untreated human neuroblastomas correlates with advanced disease stage. Science 1984;224:1121.
32. Seeger RC, Brodeur GM, Sather H, Dalton A, Siegel SE, Wong KY, et al. Association of multiple copies of the N-myc oncogene with rapid progression of neuroblastomas. N Engl J Med 1985;313:1111–6.
33. Cheung NV, Zhang J, Lu C. Association of age at diagnosis and genetic mutations in patients with neuroblastoma. JAMA 2012;307: 1062–71.
34. Valentijn LJ, Koster J, Zwijnenburg DA, Hasselt NE, van Sluis P, Volckmann R, et al. TERT rearrangements are frequent in neuroblastoma and identify aggressive tumors. Nat Genet 2015;47:1411–4.
35. Janku F, Angenendt P, Tsimberidou AM, Fu S, Naing A, Falchook GS, et al. Actionable mutations in plasma cell-free DNA in patients with advanced cancers referred for experimental targeted therapies. Oncotarget 2015; 6:12809–21.
36. Schwaederle M, Husain H, Fanta PT, Piccioni DE, Kesari S, Schwab RB, et al. Detection rate of actionable mutations in diverse cancers using a biopsy-free (blood) circulating tumor cell DNA assay. Oncotarget 2016; 7:9707–17.
37. Heitzer E, Ulz P, Belic J, Gutschi S, Quehenberger F, Fischereder K, et al. Tumor-associated copy number changes in the circulation of patients with prostate cancer identified through whole-genome sequencing. Genome Med 2013;5:30-.
38. Xia S, Kohli M, Du M, Dittmar RL, Lee A, Nandy D, et al. Plasma genetic and genomic abnormalities predict treatment response and clinical outcome in advanced prostate cancer. Oncotarget 2015;6:16411–21.
39. Vanderstichele A, Busschaert P, Smeets D, Landolfo C, Van Nieuwenhuysen E, Leunen K, et al. Chromosomal instability in cell-free DNA as a highly specific biomarker for detection of ovarian cancer in women with adnexal masses. Clin Cancer Res 2017;23:2223.
40. Taylor F, Bradford J, Woll PJ, Teare D, Cox A. Unbiased Detection of Somatic Copy Number Aberrations in cfDNA of Lung Cancer Cases and High-Risk Controls with Low Coverage Whole Genome Sequencing. In: Gahan PB, Fleischhacker M, Schmidt B, editors. Circulating Nucleic Acids in Serum and Plasma – CNAPS IX. Cham: Springer International Publishing; 2016. p29–32.
41. Cohen PA, Flowers N, Tong S, Hannan N, Pertile MD, Hui L. Abnormal plasma DNA profiles in early ovarian cancer using a non-invasive prenatal testing platform: implications for cancer screening. BMC Med 2016; 14:126.
42. Heitzer E, Auer M, Gasch C, Pichler M, Ulz P, Hoffmann EM, et al. Complex tumor genomes inferred from single circulating tumor cells by array-CGH and next-generation sequencing. Cancer Res 2013;73:2965.
43. Bettegowda C, Sausen M, Leary RJ, Kinde I, Wang Y, Agrawal N, et al. Detection of circulating tumor DNA in early- and late-stage human malignancies. Sci Transl Med 2014;6:224ra24–ra24.
44. Kang Q, Henry NL, Paoletti C, Jiang H, Vats P, Chinnaiyan AM, et al. Comparative analysis of circulating tumor DNA stability In K3EDTA, Streck, and CellSave blood collection tubes. Clin Biochem 2016;49: 1354–60.
45. Kojima M, Hiyama E, Fukuba I, Yamaoka E, Ueda Y, Onitake Y, et al. Detection of MYCN amplification using blood plasma: noninvasive therapy evaluation and prediction of prognosis in neuroblastoma. Pediatr Surg Int 2013;29:1139–45.
46. Combaret V, Hogarty MD, London WB, McGrady P, Iacono I, Brejon S, et al. Influence of neuroblastoma stage on serum-based detection of MYCN amplification. Pediatr Blood Cancer 2009;53:329–31.
47. Gotoh T, Hosoi H, Iehara T, Kuwahara Y, Osone S, Tsuchiya K, et al. Prediction of MYCN amplification in neuroblastoma using serum DNA and real-time quantitative polymerase chain reaction. J Clin Oncol 2005;23:5205–10.
48. Carén H, Erichsen J, Olsson L, Enerbäck C, Sjöberg R-M, Abrahamsson J, et al. High-resolution array copy number analyses for detection of deletion, gain, amplification and copy-neutral LOH in primary neuroblastoma tumors: Four cases of homozygous deletions of the CDKN2A gene. BMC Genomics 2008;9:353-.
49. Hindson BJ, Ness KD, Masquelier DA, Belgrader P, Heredia NJ, Makarewicz AJ, et al. High-throughput droplet digital PCR system for absolute quantitation of DNA copy number. Anal Chem 2011;83:8604–10.
50. Schmitt MW, Kennedy SR, Salk JJ, Fox EJ, Hiatt JB, Loeb LA. Detection of ultra-rare mutations by next-generation sequencing. Proc Natl Acad Sci U S A 2012;109:14508–13.
51. Eleveld TF, Oldridge DA, Bernard V, Koster J, Daage LC, Diskin SJ, et al. Relapsed neuroblastomas show frequent RAS-MAPK pathway mutations. Nat Genet 2015;47:864–71.
52. Schramm A, Koster J, Assenov Y, Althoff K, Peifer M, Mahlow E, et al. Mutational dynamics between primary and relapse neuroblastomas. Nat Genet 2015;47:872–7.